doi:10.36487/ACG_repo/2435_G-17

Pilot numerical analysis for geometry optimization of lined rock cavern

W. Luo, P. Zhang, Y. Zou and D. Johansson
Luleå University of Technology, Luleå, Sweden

ABSTRACT

Lined rock caverns are an innovative solution for underground gas storage. Inspired by the design of lined rock cavern (LRC) in Skallen, Sweden, concerns arise about potential stress concentration regions within cavern liners since they pose challenges to the long-term stability and safety of LRC. To improve the liner stability, the shape optimization of LRC was explored preliminarily through numerical modelling that included all key components, i.e., the rock mass, concrete and steel liners, and the sliding layer between them. Besides Skallen's original design, three additional steel liner shapes were proposed. Their performance under certain internal pressures was assessed based on the distribution of stress in the steel liner and displacement in the sliding layer. Due to the lack of confirmed data, two different groups of mechanical parameters of the sliding layer were compared. One set was derived through calibration, using displacement data monitored in the field within the sliding layer, while the other reflected the condition that steel liner contacts concrete liner directly. It is found that stress and shear displacement concentration typically occur at the invert corner of steel liner. This issue can be significantly mitigated by using a junction with smooth transition, such as the shape with a semi-circular bottom. Moreover, the impacts of the liner shape on the stress concentration become more pronounced when the sliding layer is more rigid. The results improve the understanding of the interaction effects between the sliding layer and steel liner, thereby enhancing the feasibility and reliability of further optimal LRC design.

1 INTRODUCTION

International efforts to enable society's energy to follow a sustainable path include replacing fossil fuels with hydrogen. This demand has led Sweden to continue to develop large-scale hydrogen storage technology. Due to the lack of natural geological formations for gas storage in Sweden, lined rock cavern (LRC) has become the last resort for underground hydrogen/gas storage.

The concept of LRC originated in Sweden in the mid-1980s. Extensive tests were conducted at a pilot plant in Grängesberg, Sweden, between 1989 and 1993 to evaluate the performance of various liners, the effect of increasing internal pressures, the benefit of reduced storage temperature, as well as the rock failure and leakage in the liner. Based on these experiences, a design method of LRC was proposed and used at LRC Demo Plant at Skallen, Sweden (Johansson 2003). Glamheden and Curtis (2006) provided a detailed description of the layout, geometry, and geology of the LRC at Skallen. One of the key considerations by using the LRC in underground gas storage is to prevent damage to the steel liner and thus avoid gas leakage. Existing studies have shown that there are large stress/strain concentrations at the chamfers of the steel liner (Johansson 2003; Damasceno 2022). It poses challenge to the long-term stability and safety of LRC.

The stress concentration in a structure primarily relies on its own shape. The shape design of underground cavern is one of the classical topics in rock engineering and has been studied by many scholars. Assuming that the rock is homogeneous and elastic, there exists an optimal shape for the cross-section of a rectangular-like underground cavern (Cristescu 1995). Wang et al. (2013) introduced the concepts of slope instability and compressive curvature in the structural design of salt caverns. The results showed that the pressure of the internal gas affects the shape design of salt caverns. Cyran and Kowalski (2021) analyzed the stability of different cavern shapes under the applied geological conditions based on numerical simulations. The results showed that the analyzed stability factors are sensitive to changes in initial cavern diameter and shape. It was also noted that shapes with sharp edges showed poorer stability than those with smooth edges. Nevertheless, while studies have focused on the response of the rock mass under different cavern shapes, there has been limited research conducted on optimizing the shape of lined rock cavern based on the performance of the steel liner.

Besides the shape of the steel liner itself, its interaction with other structural components also plays significant role in the stress distribution. Damasceno et al. (2022) demonstrated the effects of rock joints opening on the performance of the steel liner under high internal pressure using finite element models. Analytical and numerical models for predicting the response of the rock mass to high internal pressures were subsequently developed (Damasceno et al. 2023). Furthermore, a design tool that combines numerical simulation and probability analysis was proposed (Damasceno 2023). However, the sliding layer, which directly contacts the steel liner and notably influences stress distribution of the steel liner (Johansson, 2003), has not been fully taken into account. Its mechanical behavior was usually simplified in previous studies.

Correspondently, to reduce the stress concentration of the steel liner within the LRC, this paper employs numerical models to analyze its stress and displacement distribution under various proposed shapes, with the full consideration of the interactions among different LRC components. Specifically, the impacts of different mechanical parameters of the sliding layer are assessed. The objective is to establish a reference framework for optimizing the shape of the LRC.

2 LRC DEMO PLANT AT SKALLEN

The LRC Demo plant is located at Skallen near Halmstad in south-western Sweden. Following extensive demonstration and commissioning after completion in the summer of 2002, the plant entered commercial operation on the Swedish gas grid (Tengborg et al. 2014).

The shape of the storage cavern is a vertical cylinder with a spherical top and rounded semi-ellipsoid bottom. The overburden at the cavern location is 115 m thick. The cavern has a diameter of 36 m and a height of 52 m. The geometric volume of the cavern is 40 000 m^3 and it stores gas with a pressure not exceeding 23 MPa. The main structure of the LRC includes the surrounding rock, concrete liner, a sliding layer, and a steel liner (Damasceno 2022). The thicknesses of the concrete liner, steel liner and the sliding layer are 1 m, 12 mm and 6 mm, respectively.

3 NUMERICAL MODEL

Numerical models were established based on the LRC Demo plant at Skallen through software FLAC3D. Different LRC components including rock mass, concrete liner, steel liner and sliding layer were simulated in numerical models by using different elements. Solid elements were employed to simulate the surrounding rock and concrete liner, whereas liner structural elements were used to simulate the steel liner. The slider layer was considered as the interface between concrete liner and steel liner.

3.1 Model geometry and boundary conditions

As shown in Figure 1, in order to reduce the influence of boundary effects, the numerical model including LRC becomes a large cube with a side length of 200 m.

Based on the in-situ stress measurements, the in-situ stress field was evaluated by Glamheden and Curtis (2006). The magnitude of the in-situ stresses versus depth listed in Table 1 were assigned in the numerical model, where the major horizontal principal stress is parallel to the

Y axis, minor principal horizontal stress is parallel to the *X* axis and the vertical stress is parallel to the *Z* axis of the numerical models. The top of the model is the ground surface and is free of constraint. Roller boundaries were applied on the four sides of the model. Fixed constraints were applied to the bottom of numerical model.

Table 1 In-situ stress conditions around the cavern (Glamheden and Curtis 2006)

	Value	Unit
Major horizontal stress	$0.061z-0.32$	MPa
Minor horizontal stress	$0.0295z-0.1063$	MPa
Vertical stress	$0.0265z$	MPa

(Note: *z* means the depth in the numerical model)

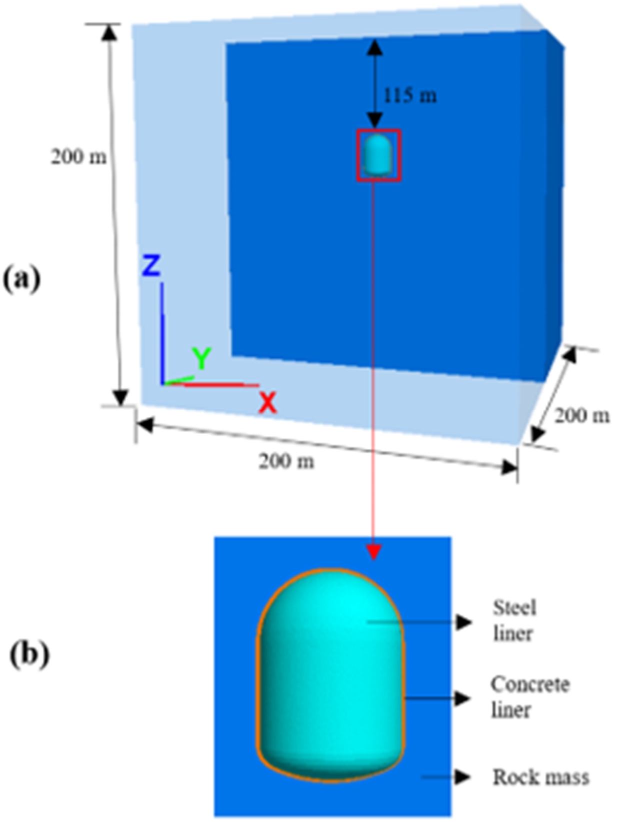

Figure 1 Schematic diagram of the three-dimensional numerical model: (a) model dimension; and (b) the major components of LRC.

To simulate the interaction of structural components of LRC in operational phase, the entire cavern was firstly excavated, then concrete liner and steel liner were applied, and finally the gas pressure was applied to the steel liner.

3.2 Constitutive model and parameters

An ideal elastic-plastic constitutive model was used for both the rock mass and concrete liner, while an elastic constitutive model was utilized for the steel liner. The parameters of these components were set to align with the specifications provided in Itasca's report, as outlined in Table 2 (Damjanac et al. 2002).

Table 2 Parameters of rock mass, concrete liner and steel liner

	Parameters	Value	Unit
Rock mass	Density	2400	kg/m^3
	Elastic modulus	36	GPa
	Poisson's ratio	0.2	
	Cohesion	13.4	MPa
	Tensile strength	5.04	MPa
	Friction angle	34	°
	Dilation angle	7	°
Concrete liner	Density	2400	kg/m^3
	Bulk modulus	16.7	GPa
	Shear modulus	12.5	GPa
	Cohesion	9.6	MPa
	Friction angle	45	°
	Tension strength	2.7	MPa
Steel liner	Elastic Modulus	200	GPa
	Poisson's ratio	0.3	
	Density	8000	kg/m^3

To model the sliding layer between the concrete and steel liners, which has been noted to significantly influence stress distribution

(Johansson 2003), a structural link deformable model was employed. To facilitate sliding and/or opening of the liner elements relative to the zone surfaces, zero tensile strength and cohesion were assumed. The friction coefficient was set to 0.1, consistent with laboratory tests using bitumen as the sliding layer material (Johansson 2003).

The stiffness of sliding layer usually made of bitumen varies with layer thickness, temperature, and pressure, posing challenges in determining its value over the entire hydrogen storage period. Two cases were discussed:

1. Case I involved estimating shear and normal stiffnesses through trail-and-error calibrations based on sliding layer deformation monitored by Johansson (2003).

2. Case II considered the liner-zone interface to be stiff compared to the surrounding material, with normal and shear stiffnesses estimated according to recommendations from Itasca Consulting Group, Inc. (2023).

The properties of the sliding layers in these two cases are detailed in Table 3.

Table 3 Parameters of sliding layer

Cases	Parameters	Value	Unit
I	Normal stiffness	45	GPa/m
	Shear stiffness	43	MPa/m
	Friction coefficient	0.1	-
	Tensile strength	0	MPa
	Cohesion	0	MPa
II	Normal stiffness	167	GPa/m
	Shear stiffness	167	GPa/m
	Friction coefficient	0.1	-
	Tensile strength	0	MPa
	Cohesion	0	MPa

3.3 Studied shapes

To explore the impact of cavern internal shape on the stability of the steel liner, simulations were conducted for four different shapes, as illustrated in Figure 2, using the parameters specified in the aforementioned two cases. The primary distinction among the four shapes lies in the variation of their bottom contours. Their bases are as follows:

a) Semi-elliptical: Simulating the original shape of the LRC used at Skallen.

b) Arc-shaped: Simulating the scenario where the transition between the middle cylinder and the bottom is not smooth.

c) Rounded flat arch: Simulating the situation where the volume of the excavated cavern is fully utilized, i.e. the largest.

d) Semi-circle: Proposed based on the analysis of the results from the first three cases, aiming to minimize stress and strain concentration on the LRC structure.

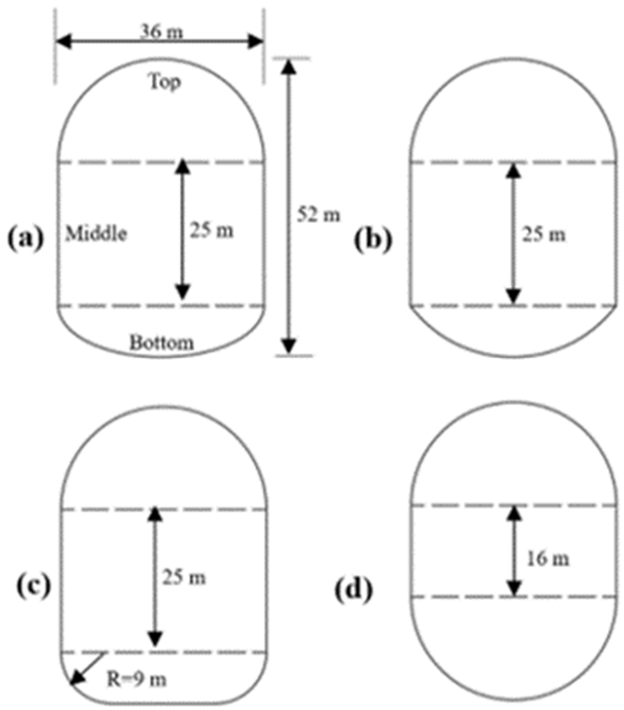

Figure 2 Vertical section of LRC.

4 RESULTS AND ANALYSIS

According to the results, it is found that the stress concentration appears at two areas. The first area is at the middle section of the cylindrical part, which is designated by section A-A, hereafter referred to as the middle area. The second area is at the connecting area between the middle and the bottom parts, designated by the B-B section, called the invert corner.

Since the pressure inside the steel liner is greater than the ground stress, the entire steel liner is in a state of outward expansion. Therefore, the focus of the stress analysis is placed on the minor principal stresses in the steel liner. It should be noted that tensile stress is positive in FLAC3D. The distribution of the minor principal stress under different scenarios is plotted in Figure 3.

The normal displacement and shear displacement of the sliding layer are read through the FISH function and then displayed through contours as shown in Figure 4 and Figure 5, respectively. The negative sign of the normal displacement of the sliding layer indicates the outward expansion of the steel liner.

4.1 Results from cavern Shape 1 in Case I

The initial analysis focused on the results from cavern Shape 1 in Case I, representing the original scenario. As depicted in Figure 3(a), it is evident that the stress redistributions are uneven in both the middle area and invert corner. The maximum values at sections A-A and B-B are 195 MPa and 176 MPa, respectively.

In the first figure in Figure 4(a), it is noticeable that the normal displacement of the sliding layer at the invert corner is relatively smaller compared to other locations. However, the shear displacement of the sliding layer is obviously concentrated at the invert corner, as depicted in Figure 5(a).

4.2 Effect of sliding layer

Comparing the stress distribution in the steel liner of the two cases, as illustrated in Figure 3, it can be found that when the stiffness of the sliding layer is higher, the maximum tensile stresses at both sections in Case II surpass those in Case I. Moreover, the maximum values at the invert corners become larger than those in the middle sections, contrary to what is observed in Case I.

As the stiffness of the sliding layer increases, there is a noticeable decrease in both normal and shear displacements, as illustrated in Figures 4 and 5. Nevertheless, the pattern of displacement distribution remains consistent across different stiffness levels. Specifically, the smallest normal displacement occurs at the invert corner, whereas the shear displacement is primarily concentrated at the same location.

4.3 Effect of cavern shape

Considering the changes in the shape of the cavern would have different effects on the response of the steel liner under different sliding layer parameters, the effects of changes in the shape of the cavern in Case I and Case II are analyzed separately.

4.3.1 Case I

As shown in Figure 3(a), the maximum tensile stresses in the middle area are higher than those in the invert corner. The values decrease in the following order: Shape 3 > Shape 1 > Shape 2 > Shape 4.

Figure 4(a) shows that the maximum values of normal displacement are identical across different shapes. This consistency can be attributed to the fact that the normal displacement at the invert corner is the smallest in each scenario. Changes in the shape at the invert corner have minimal impact on the maximum values but do influence the minimum values.

Figure 5(a) presents the shear displacement of the sliding layer for Case I. For Shape 1 and Shape 2, there is a pronounced concentration at the invert corner. In Shape 3, this concentration phenomenon occurs at the bottom near the invert corner. Shape 4 shows only a slight concentration in the middle area and at the invert corner. According to the maximum shear displacement of each shape, they rank from largest to smallest as follows: Shape 2 > Shape 1 > Shape 3 > Shape 4.

4.3.2 Case II

Figure 3(b) for Case II reveals tensile stress concentrations in the middle area and at the invert corner of the steel liner. Unlike Case I, the maximum value in the middle area is smaller than that at the invert corner, emphasizing a more pronounced concentration at the invert corner. Regarding the maximum tensile stress for each shape, the values rank from largest to smallest as follows: Shape 2 > Shape 3 > Shape 1 > Shape 4. Moreover, from the comparison between Figure 3(a) and (b), it is notable that the impacts of the liner shape on the stress concentration become more significant when the sliding layer is more rigid.

Figure 4(b) shows that the distribution of normal displacement in the sliding layer for Case II is similar to that in Case I. However, since the normal stiffness of the sliding layer in case II is larger, the normal displacement values are smaller in comparison.

Figure 5(b), depicting Case II, also shows that the shear displacements of the sliding layer exhibit patterns similar to those in Case I, though with smaller magnitudes. Additionally, by comparing Figure 5(a) and (b), it can be found that the impacts of the liner shape on the shear displacement concentration become more pronounced when the sliding layer is less rigid.

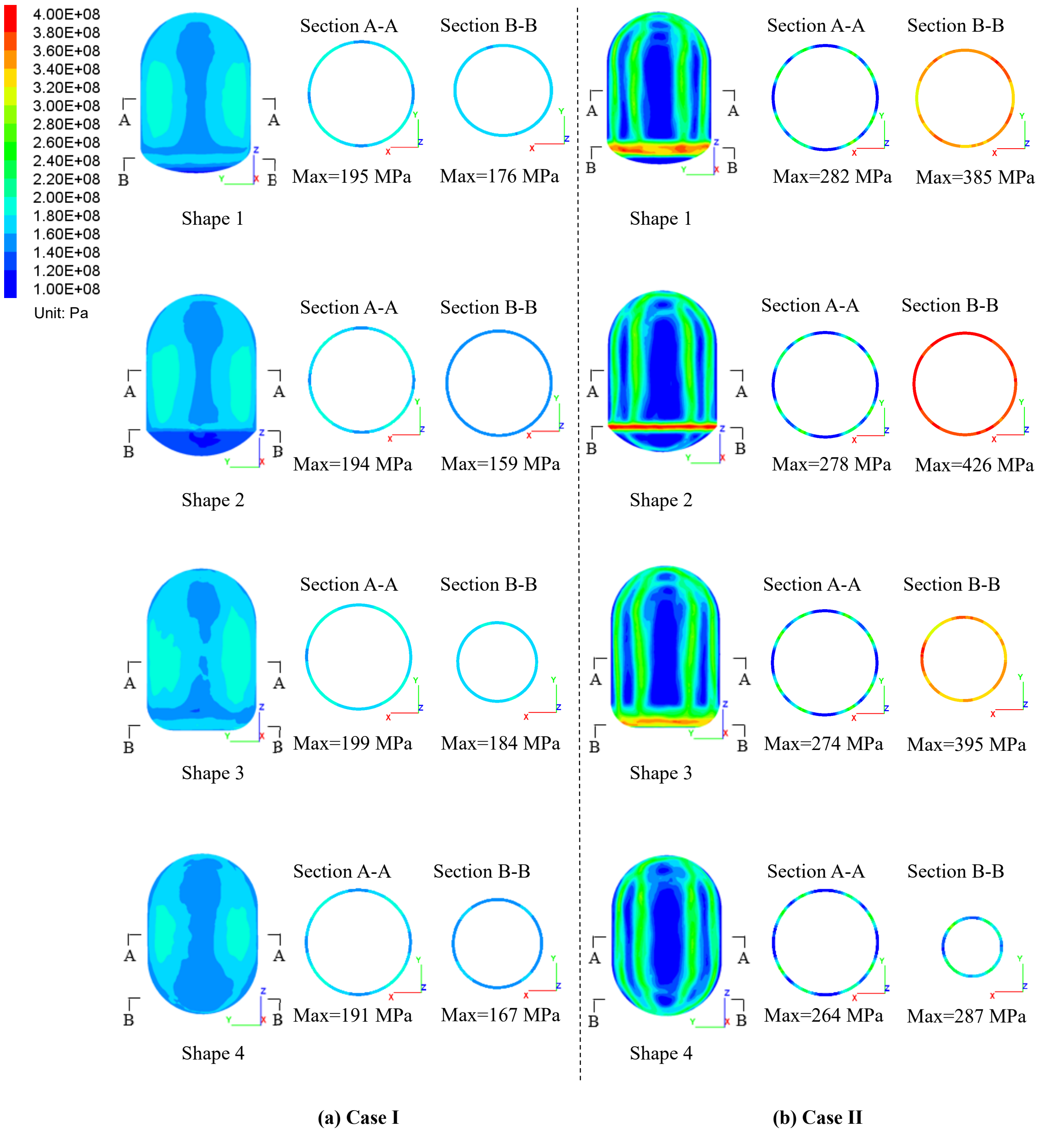

Figure 3 Minor principal stress of steel liner.

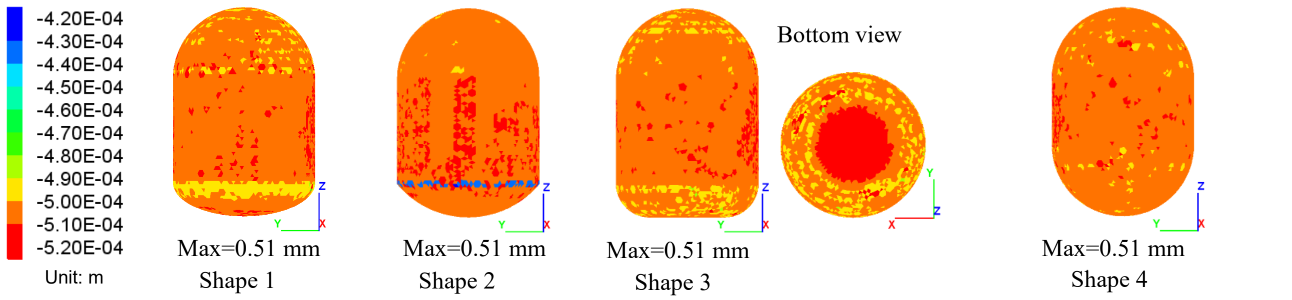

(a) Case I

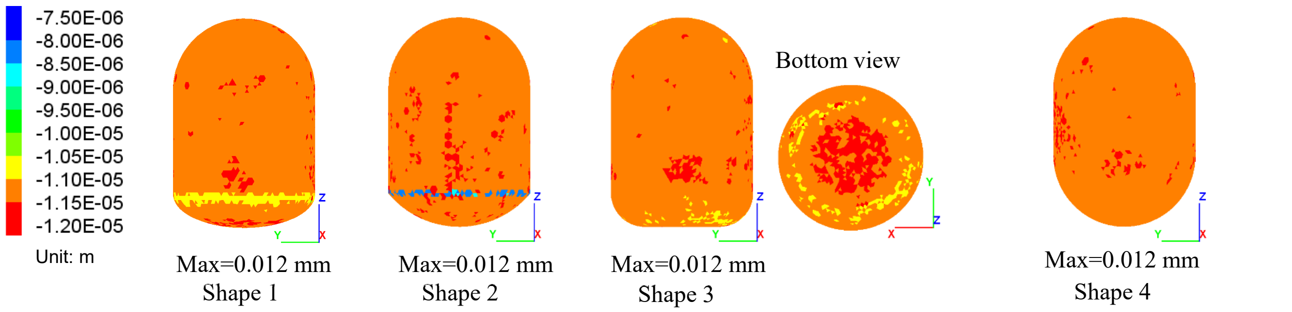

(b) Case II

Figure 4 Normal displacement of sliding layer.

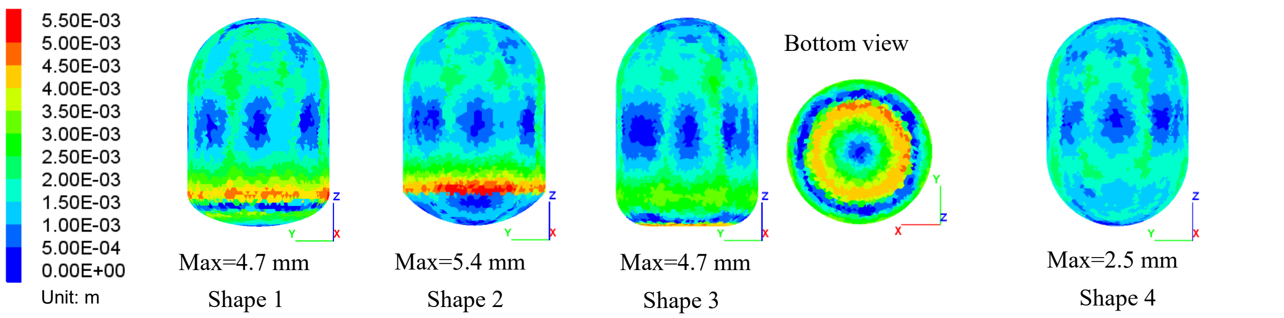

(a) Case I

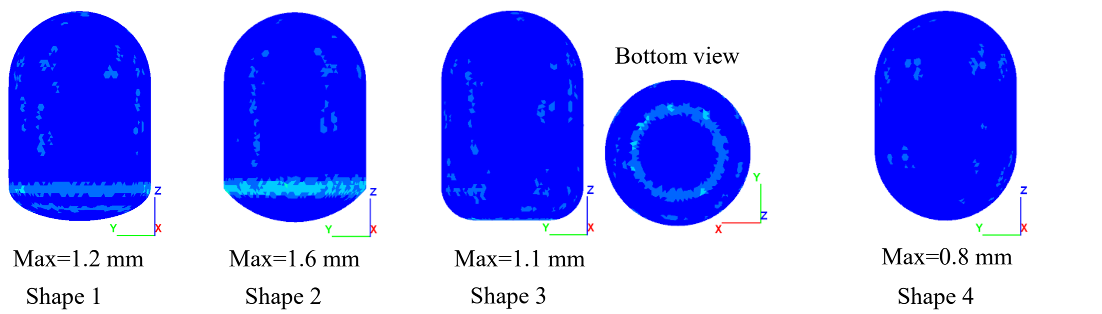

(b) Case II

Figure 5 Shear displacement of sliding layer.

5 DISCUSSION AND CONCLUDING REMARKS

As LRC is used for gas storage, it requires a long service life. Unlike unlined caverns, LRCs incorporate structural components such as concrete liners, sliding layers and steel liners.

The interaction between different components, as well as the geometric and mechanical properties of the components has great influence on the performance of LRC. Based on the numerical study, the following conclusions can be drawn.

(a) The results for the original shape (Shape 1) under Case I indicate that the concentration of the minor principal stress on the steel liner is more pronounced in the middle area compared to the invert corner. The smallest normal displacement is observed at the invert corner, whereas the largest shear displacement is primarily concentrated at the same location.

(b) Comparing the results of Case I and Case II reveals that with the increased stiffness of the sliding layer, the stress concentration at the invert corner becomes more pronounced and exhibits more significant variations across different shapes. Conversely, a softer sliding layer significantly reduces stress concentration. However, this also leads to a marked increase in displacement within the sliding layer, particularly with shear displacement being notably concentrated at the invert corner. This underscores the importance of ensuring that the sliding layer has the appropriate mechanical properties to simultaneously keep both stress and displacement within acceptable limits.

(c) The bottom shape of LRC has a significant impact on their mechanical performance. Based on this study, the optimum shape is semi-circle (Shape 4), which exhibiting less concentration in both the minor principal stress and the shear displacement. On the other hand, the volume being used for storing gas becomes the smallest for this shape. The optimization of LRC design should attempt to reach the optimum mechanical performance and storage capacity, which is being investigated in current work.

ACKNOWLEDGEMENT

The work has been carried out within the project "Hydrogen, ammonia, and methanol in hydrogen hubs in the Nordic region" with the acronym H2AMN to the Council of Ministers, Nordic Energy Research (NER) (project no. 2315912-0611). The authors gratefully acknowledge the funding from this project and CH2ESS, Luleå University of Technology, Sweden.

REFERENCES

Cristescu, N. D. & Paraschiv, I. (1995). The optimal shape of rectangular-like caverns. In *International Journal of Rock Mechanics and Mining Sciences & Geomechanics Abstracts*, 32 (4): 285-300.

Cyran, K. & Kowalski, M. (2021). Shape modelling and volume optimisation of salt caverns for energy storage. *Applied Sciences*, 11(1): 1-24.

Damasceno, D. R. (2022). Modeling aspects of reliability-based design of lined rock caverns. Ph.D. thesis, Royal Institute of Technology (KTH), Stockholm, Sweden, 85 p.

Damasceno, D. R., Spross, J. & Johansson, F. (2023). Effect of rock joints on lined rock caverns subjected to high internal gas pressure. *Journal of Rock Mechanics and Geotechnical Engineering*, 15(7): 1625-1635.

Damasceno, D. R., Spross, J. & Johansson, F. (2023). Rock mass response for lined rock caverns subjected to high internal gas pressure. *Journal of Rock Mechanics and Geotechnical Engineering*, 15(1): 119-129.

Damjanac, B., Carranza-Torres, C. & Dexter, R. (2002). Technical review of the LRC concept and design methodology – Steel liner response (Report No. DE-AM26-99FT40463). Itasca Consulting Group.

Glamheden, R. & Curtis, P. (2006). Excavation of a cavern for high-pressure storage of natural gas. *Tunnelling and Underground Space Technology*, 21(1): 56-67.

Itasca Consulting Group, Inc. (2023). FLAC3D — Fast Lagrangian Analysis of Continua in Three-Dimensions, Ver. 9.0. Minneapolis: Itasca.

Johansson, J. (2003). Cavern wall design principles. Licentiate thesis, Royal Institute of Technology (KTH), Stockholm, Sweden, 139 p.

Tengborg, P., Johansson, J. G. D. J. & Durup, J. G. (2014). Storage of highly compressed gases in underground Lined Rock Caverns–More than 10 years of experience. In Proceedings of the world tunnel congress. 1-7 May 2014, Foz do Iguaçu, Brazil.

Wang, T., Yan, X., Yang, H., Yang, X., Jiang, T. & Zhao, S. 2013. A new shape design method of salt cavern used as underground gas storage. *Applied Energy*, 104: 50-61.